Hindawi Publishing Corporation
Bioinorganic Chemistry and Applications
Volume 2013, Article ID 439848, 11 pages
http://dx.doi.org/10.1155/2013/439848

Research Article

Cu(II), Ni(II), and Zn(II) Complexes of Salan-Type Ligand Containing Ester Groups: Synthesis, Characterization, Electrochemical Properties, and *In Vitro* Biological Activities

P. Jeslin Kanaga Inba, B. Annaraj, S. Thalamuthu, and M. A. Neelakantan

Chemistry Research Centre, National Engineering College, K.R. Nagar, Kovilpatti, Thoothukudi District, Tamil Nadu 628 503, India

Correspondence should be addressed to M. A. Neelakantan; drmaneelakantan@gmail.com

Received 10 April 2013; Accepted 20 June 2013

Academic Editor: Spyros Perlepes

A salen ligand on reduction and N-alkylation affords a novel [N_2O_2] chelating ligand containing ester groups [L = diethyl-2,2′-(propane-1,3-diylbis((2-hydroxy-3-methoxy benzyl)azanediyl))diacetate]. The purity of the ligand was confirmed by NMR and HPLC chromatograms. Its Cu(II), Ni(II), and Zn(II) complexes were synthesized and characterized by a combination of elemental analysis, IR, NMR, UV-Vis, and mass spectral data, and thermogravimetric analysis (TG/DTA). The magnetic moments, UV-Vis, and EPR spectral studies support square planar geometry around the Cu(II) and Ni(II) ions. A tetrahedral geometry is observed in four-coordinate zinc with bulky N-alkylated salan ligand. The redox properties of the copper complex were examined in DMSO by cyclic voltammetry. The voltammograms show quasireversible process. The interaction of metal complexes with CT DNA was investigated by UV-Vis absorption titration, ethidium bromide displacement assay, cyclic voltammetry methods, and agarose gel electrophoresis. The apparent binding constant values suggest moderate intercalative binding modes between the complexes and DNA. The *in vitro* antioxidant and antimicrobial potentials of the synthesized compounds were also determined.

1. Introduction

Salen metal complexes are the interest of many workers because of their applications in food industry, in the treatment of cancer [1], as antibactericide agents [2, 3], as antivirus agents [4], as fungicide agents [5], and for other biological properties [6]. The antitumor activity of salen complex arises due to its DNA binding properties. The salen complexes are conformationally flexible and adopt a variety of geometries. Also, salen metal complexes have a unique flat electron-rich aromatic surface that may facilitate their interactions with nucleic acids. Hydroxyl groups in the salen complexes act as a quinone system which would cooperate to facilitate the formation of free radicals responsible for DNA cleavage [7]. The biological properties of salen complexes are enhanced by functionalization with a variety of substituents [8–11]. When salen compounds are reduced at the imine function, the more flexible, reduced salen derivatives (salan) are obtained.

Considerable attention has been devoted to the preparation and structural characterization of metal complexes containing salen-type ligands. However, little attention has been paid to systems in which functionalized salan is used as ligands. In the present investigation N-alkylated salan complexes are used for DNA binding and antimicrobial and antioxidant properties. In continuation of our earlier works on salen-type ligands [12–14], the present investigation reports on the synthesis and spectral characterization of Cu(II), Ni(II), and Zn(II) complexes with N-alkylated salan ligand. The interaction of the metal complexes with calf thymus (CT) DNA was studied by UV-Vis and fluorescence spectroscopy and cyclic voltammetric method. The DNA cleaving nature of the compounds was tested against pUC19 DNA in the absence and presence of hydrogen peroxide. The *in vitro* antimicrobial activity of the compounds was assessed against various microorganisms. The antioxidant activity of the metal complexes was investigated systematically.

2. Experimental

2.1. Materials and Methods. All chemicals employed for the synthesis were of analytical reagent grade and of highest purity available. *o*-Vanillin and 1,3-diaminopropane were purchased from Sigma Aldrich and used as received. Solvents used for spectroscopic and electrochemical studies were purified and dried by standard procedures [15]. Metal acetates were purchased from Merck. CT DNA and pUC19 DNA were purchased from GeNei, Bangalore, and used without purification. Tris-(hydroxylmethyl)-aminomethane-HCl (Tris-HCl) and ethidium bromide (EB) were obtained from HiMedia. Tris-HCl-NaCl buffer solution was prepared with double-distilled water. Tetrabutylammonium perchlorate (TBAP) was used as a supporting electrolyte for recording cyclic voltammograms.

2.2. Physical Measurements. Elemental analyses were recorded on a Thermo Finnigan Flash EA 1112 elemental analyzer. Molar conductance values of the complexes in DMSO were obtained on a Systronics Model 611 digital conductivity meter. Magnetic susceptibility measurements on powder samples were carried out on a Gouy balance at room temperature using mercuric tetra(thiocyanato)cobaltate (II) as the calibrant. The infrared (IR), ultraviolet-visible (UV-Vis), and emission spectra were recorded on Shimadzu 8400 S, Shimadzu UV-2450, and Shimadzu RF-5301 PC spectrophotometers, respectively. The ^{1}H and ^{13}C NMR of ligand in $CDCl_3$ and zinc complex in DMSO-d_6 were recorded on Bruker AV 300 MHz spectrophotometer. Electrospray ionization (ESI) mass spectral measurements were recorded on Micromass Quattro II mass spectrometer. Electron paramagnetic resonance (EPR) spectrum of the Cu complex in DMSO solution was recorded on JES-FA200 spectrometer at 300 K and at 77 K using tetracyanoethylene (TCNE, g = 2.00277) as the g marker. The thermogravimetric analysis/differential thermal analysis (TGA/DTA) was carried out in dynamic nitrogen atmosphere with a heating rate of 20°C/min using NETZSCH STA 449F3 thermal analyzer. Cyclic voltammograms were recorded on a CHI 603 C electrochemical analyzer with a three-electrode compartment.

2.3. Synthesis of the Ligand (L). The synthetic procedure of the ligand was reported in our earlier work [14]. Color: yellow oil. Yield: 60%; Analytical data. Calculated data, for [$C_{27}H_{38}N_2O_8$] (%): C, 62.53; H, 7.38; N, 5.40. Found (%): C, 62.67; H, 7.25; N, 5.48. IR (cm^{-1}): 1273 (phenolic –C–O), 1195 (–C–N), and 1747 ester (–C=O). ^{1}H NMR ($CDCl_3$): 4.16 (H9, 4H), 3.86 (H5, H11, 10H), 3.35 (H8, 4H), 6.58–6.87 (aromatic-H, 6H), 2.63 (H6, 4H), and 1.77 (H7, 2H) δ. λ_{max} in CH_3OH, 267, 333 nm.

2.4. Synthesis of the Metal Complexes. The metal complexes were isolated as follows: metal acetate (2 mmol) dissolved in 10 mL of methanol was added dropwise to a 10 mL methanolic solution of the ligand (2 mmol). The mixture was kept under reflux for 1-2 hours. The solution thus obtained gave the compound on concentration and cooling. All the compounds are soluble in DMSO. The yields were around 70–80%. The synthesis is given in Scheme 1. For the crystallization, the compounds were dissolved in different solvent mixtures and evaporated slowly at room temperature. But our attempts to crystallize the compounds were unsuccessful.

2.4.1. [CuL]·H_2O. Colour: dark brown; anal. calcd for [Cu($C_{27}H_{36}N_2O_8$)]·H_2O (%): C, 54.22; H, 6.40; N, 4.68; Cu, 10.62. Found (%): C, 54.35; H, 6.45; N, 4.76; Cu, 10.67. IR (cm^{-1}): 1265 (phenolic –C–O), 1181 (–C–N), 1749 (–C=O in ester group), 584 (M–N), and 461 (M–O). *m/z*: 580. λ_{max} in DMSO 285, 349, and 527 nm. μ_{eff}: 1.85 BM. Λ_m: 12.72 mho cm^2 mol^{-1}.

2.4.2. [NiL]·H_2O. Colour: red; anal. calcd for [Ni($C_{27}H_{36}N_2O_8$)]·H_2O (%): C, 54.66; H, 6.46; N, 4.72; Ni, 9.89. Found (%): C, 54.71; H, 6.50; N, 4.65; Ni, 9.97. IR (cm^{-1}): 1261 (phenolic –C–O), 1187 (–C–N), 1747 (–C=O in ester group), 551 (M–N), and 470 (M–O). ^{1}H NMR (DMSO-d_6): 4.21 (H9, 4H), 3.91 (H11, 6H), 4.37 (H5, 4H), 3.70 (H8, 4H), 6.57–6.94 (aromatic-H, 6H), 3.20 (H6, 4H), and 1.85 (H7, 2H) δ. *m/z*: 575. λ_{max} in DMSO 280, 345, and 553 nm. Λ_m: 11.56 mho cm^2 mol^{-1}.

2.4.3. [ZnL]·H_2O. Colour: pale yellow; anal. calcd for [Zn($C_{27}H_{36}N_2O_8$)]·H_2O (%): C, 54.05; H, 6.38; N, 4.67; Zn, 10.90. Found (%): C, 54.12; H, 6.46; N, 4.81; Zn, 10.97. IR (cm^{-1}): 1267 (phenolic –C–O), 1183 (–C–N), 1749 (–C=O in ester group), 547 (M–N), and 451 (M–O). ^{1}H NMR (DMSO-d_6): 4.19 (H9, 4H), 3.92 (H11, 6H), 4.35 (H5, 4H), 3.72 (H8, 4H), 6.55–6.91 (aromatic-H, 6H), 3.16 (H6, 4H), and 1.79 (H7, 2H) δ. *m/z*: 582. λ_{max} in DMSO 282 and 350 nm. Λ_m: 13.28 mho cm^2 mol^{-1}.

2.5. DNA Binding Experiments

2.5.1. UV-Vis Spectroscopic Studies. The DNA binding experiments were performed at room temperature. A solution of CT DNA in the buffer (5 mM Tris-HCl and 50 mM NaCl) gave a ratio of UV absorbance at 260 and 280 nm of about 1.8–1.9 : 1, indicating that the CT DNA was sufficiently free from protein [16]. The concentration of DNA was measured using its extinction coefficient at 260 nm (6600 mol L^{-1} cm^{-1}) [17]. Concentrated stock solutions of the compounds in DMSO were prepared and diluted suitably with the buffer to the required concentrations for all the experiments. The absorption titrations of the compounds in buffer were performed using a fixed concentration (10 μM) to which increments of the DNA stock solution were added (R = [DNA]/[complex] = 0, 2, 4, 6, 8, and 10). Compound DNA solutions were allowed to incubate for 30 min before the spectra were recorded. From the absorption data, the intrinsic binding constant, K_b, was determined using the following [18]:

$$\frac{[\mathrm{DNA}]}{(\varepsilon_a - \varepsilon_f)} = \frac{[\mathrm{DNA}]}{(\varepsilon_b - \varepsilon_f)} + \frac{1}{K_b(\varepsilon_b - \varepsilon_f)}, \quad (1)$$

where ε_a, ε_f, and ε_b are the apparent, free, and bound compound extinction coefficients, respectively. In the plots

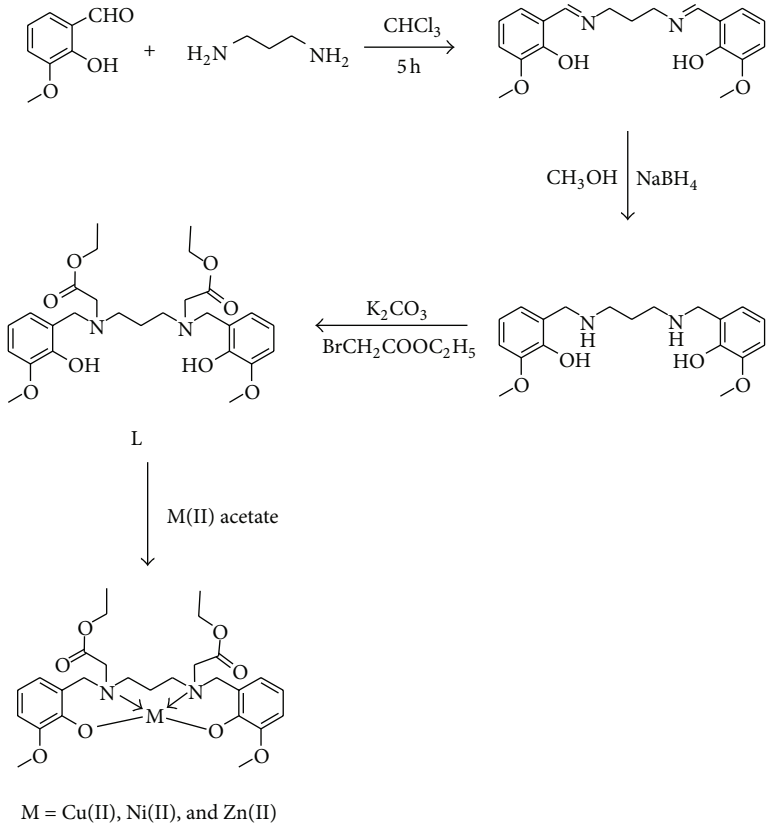

Scheme 1: Synthesis route for ligand and metal complexes.

of [DNA]/($\varepsilon_a - \varepsilon_f$) versus [DNA], K_b is given by the ratio of slope to the intercept.

2.5.2. Fluorescence Studies. The interaction of the synthesized compounds with DNA was further studied by ethidium bromide (EB) displacement method. The excitation wavelength was fixed at 530 nm, and the emission range was adjusted before measurements. The changes in the fluorescence intensities at 595 nm of EB-bound CT DNA in Tris-HCl buffer (pH 7.2) were measured with respect to different concentrations of the compounds (0–120 μM). The magnitude of the binding strength of the compounds with CT DNA can be calculated using linear Stern-Volmer equation [19]:

$$\frac{I_0}{I} = 1 + K_{sv}[Q], \quad (2)$$

where I_0 and I are the fluorescence intensities of EB-DNA in the absence and presence of quencher, respectively, Q is the concentration of metal complex, and K_{sv} is linear Stern-Volmer quenching constant. The relative binding tendency of the complex to CT DNA was determined by the comparison of the slope of the line in the fluorescence intensity versus complex concentration plot. The apparent binding constant (K_{app}) was calculated using the equation $K_{app} = K_{EB}$[EB]/[complex], where [complex] is the concentration of the complex at which there is 50% reduction in the fluorescence intensity of EB, $K_{EB} = 1.0 \times 10^7\ M^{-1}$, and [EB] = 5 μM [20].

2.5.3. Electrochemical Studies. The cyclic voltammetric studies of the copper complex were performed with a three-electrode system of glassy carbon as working electrode, Pt wire as auxiliary electrode, and Ag/AgCl as reference electrode. The supporting electrolyte is 0.05 M TBAP in DMSO solution. The cell was maintained oxygen-free by passing dry nitrogen through the solution. The interaction of the copper complex with CT DNA has been investigated by monitoring the changes observed in the cyclic voltammogram of CuL in buffer (5 mM Tris-HCl/50 mM NaCl) with increasing amount of DNA.

2.6. DNA Cleavage Experiment. The DNA cleavage experiment was conducted by gel electrophoresis on pUC19 DNA. The reaction mixture was prepared as follows: 1 μL of pUC19 DNA, 5 μL of the compound in DMSO, and 1 μL of H_2O_2 followed by dilution with buffer (50 mM Tris-HCl and 50 mM NaCl) to a total volume of 25 μL. The reaction mixture was incubated at 37°C for 1 h. The 1% agarose gel was prepared and stained using ethidium bromide. The samples were then loaded on gel after mixing with 3 μL of loading dye (0.25% bromophenol and 40% sucrose). The gel was electrophoresed at 100 V using Tris-boric acid-EDTA buffer (pH = 8.0) until the bromophenol blue reached one-third of the gel.

The bands were visualized and photographed under a UV transilluminator. The experiment was also carried out in the absence of H_2O_2.

2.7. Antioxidant Property. 2,2′-diphenyl-1-picrylhydrazyl (DPPH•) scavenging capacity (antioxidant activity) was measured according to the following procedure [21, 22]. The concentration of DPPH• used for antioxidant activity was 50 μM. Different concentration of the ligand and metal complexes in methanol was added to DPPH• in methanol solution and kept at room temperature for 30 min in dark. The reduction of the DPPH• was monitored by observing the decrease in absorbance at 517 nm using UV-Vis spectrophotometer. The radical scavenging capacity of the antioxidant was expressed in terms of % inhibition and IC_{50}. The capability to scavenge the DPPH• was calculated using the following [23]:

$$\%\ \text{Inhibition} = \left(\frac{A_0 - A_{\text{sample}}}{A_0}\right) \times 100, \tag{3}$$

where A_0 is the absorbance of DPPH• in methanol solution without an antioxidant and A_{sample} is the absorbance of DPPH• in the presence of an antioxidant. The IC_{50} value is the concentration of the antioxidant required to scavenge 50% DPPH• and is calculated from the inhibition curve.

2.8. Antimicrobial Activity. All the synthesized compounds were screened for their antibacterial activity against gram-positive bacteria: *Streptococcus pyogenes* and *Staphylococcus aureus*, and gram-negative bacteria: *Escherichia coli*, *Klebsiella mobilis, Aeromonas aquariorum*, and *Serratia marcescens*, by well diffusion method [24]. Standard antibiotics, ampicillin and amoxicillin, were used as controls. Stock solutions of tested compounds were prepared in DMSO to a final concentration of 10 mg mL^{-1}. 20 mL of sterilized agar media was poured into each presterilized Petri dish and allowed to solidify by placing it in an incubator at 37°C for an hour. 24 h culture suspension was poured and neatly swabbed with the presterilized cotton swabs. Then holes of 5 mm diameter were punched carefully using a sterile cork borer, and these wells were completely filled with the prepared L or the metal complex solutions (50 μL). These dishes were transferred to an incubator maintained at 37°C for 24 h. During this period, the test solution diffused and the growth of the inoculated microorganism was affected. The inhibition zone was developed and measured at the end of the incubation period. Experiments were performed in triplicate, and standard deviation was calculated.

3. Results and Discussion

The ligand was synthesized by three steps. In the first step Schiff's base was obtained by the condensation of o-vanillin with 1,3-diaminopropane. The Schiff base was reduced using sodium borohydride in the second step. Finally ester compound is obtained by N-alkylation reaction using 2-bromoethylacetate in the presence of potassium carbonate. The ester compound obtained as yellow oily substance on complexation with metal ions forms powdered metal complexes.

3.1. Molar Conductance. The molar conductance of the synthesized metal complexes was measured in DMSO at 10^{-3} M solution. The values were found to be in the range of 12.72–16.56 mho cm^2 mol^{-1} suggesting the nonelectrolytic nature of the complexes.

3.2. IR Spectra. The ligand (L) has two characteristically strong bands (1747 and 1205 cm^{-1}) arising from C=O and C(O)–O stretching vibrations of ester groups (Figure S1) (see Supplementary Material available online at http://dx.doi.org/10.1155/2013/439848). These vibrations are unchanged in the spectra of the complexes indicating that the ester group of L is not involved in complexation with metal ion. The ligand shows two bands at 1379 and 1280 cm^{-1} corresponding to O–H bending and C–O stretching vibrations of phenolic OH group. The disappearance of O–H bending and higher shifting of C–O stretching vibrations are observed in the spectra of metal complexes suggesting that the phenolic OH group of L is involved in coordination with metal ion after deprotonation. The band at 1193 cm^{-1} assigned for C–N stretching in the free ligand is shifted to lower wave number in complexes. This suggests that the tertiary nitrogen atom of the ligand is involved in coordination with the metal ions. In all the complexes, a broad band that appears in the region 3400–3500 cm^{-1} shows the existence of uncoordinated water molecule. New bands which are not present in the ligand appeared in the ranges 505–584 cm^{-1} and 450–470 cm^{-1} in the complexes attributed to $\nu_{(M-N)}$ and $\nu_{(M-O)}$ vibrations, respectively. From the spectral data, the ligand coordinates to the metal ion through phenolic –O and tertiary –N atoms.

3.3. NMR Spectra. Formation of nickel and zinc complex is confirmed by comparing the ^{1}H NMR of ligand and its metal complex (Table S1). The N-methylene protons (H8) of ester part of L give the singlet at 3.35 δ. The methylene protons (H6) α to amino part of L show the signal at 2.63 δ. The sharp singlet at 3.86 δ corresponds to methylene protons (H5) α to phenyl ring (Figure S2). These methylene proton signals undergo higher deshielding up to 0.1 to 0.5 δ. This demonstrates that the tertiary amine nitrogen is involved in coordination with metal ion. The ligand shows that multiple signals at 4.16 and 1.43 δ are assignable to methylene and methyl protons of ester groups. These signals are not altered in the metal complex (Table S1). This suggests that the ester group of L is free from coordination with the metal ions. The aromatic protons of L show multiple signals in the region 6.58–6.87 δ. The sharp singlet at 3.86 δ corresponds to methoxy protons. These protons undergo smaller deshielding up to 0.06 δ.

The ^{13}C NMR spectral data of L is compared with its ZnL complex (Figure S3 and Figure 1). The ^{13}C NMR signal for ester group of L (C-9) is not altered in the zinc complex (Table S2). This suggests that the ester group of L is free from coordination with the metal ion. The signals for carbon atoms

adjacent to nitrogen (C-7 and C-13) are observed at 54.20 and 45.37 δ, respectively. These signals are shifted to lower value in the metal complexes. Similarly, the carbon atom adjacent to phenolic oxygen (C-1) of L is shifted to higher value in the ZnL complex. The shifts in the positions of the carbon atoms adjacent to nitrogen and phenolic oxygen clearly demonstrate the bonding of the two nitrogen atoms of tertiary amine and two oxygen atoms of phenol to the Zn(II) ion forming tetrahedral geometry.

3.4. Electronic Absorption Spectra. The UV-Vis absorption spectra of L and its metal complexes in DMSO were recorded at room temperature (Figure S4). The absorption spectrum of L shows bands at 267 and 335 nm, which are due to $\pi \rightarrow \pi^*$ transitions of phenyl ring and H-bonding induced changes of OH proton-donor aromatic molecules and amine NH (intraligand charge transfer band), respectively. The spectrum of CuL (Figure S5) displaying the band at 527 nm is assigned to $^2B_{1g} \rightarrow {}^2A_{1g}$ transition confirming the square planar geometry of the CuL (Table 1). The magnetic moment value for CuL (1.85 BM) is consistent with the square planar Cu(II) system. The NiL complex showed absorption at 553 nm ascribed to d-d transition ($^1A_{1g} \rightarrow {}^1A_{2g}$) which supports the square planar geometry around Ni(II) ion [25].

3.5. Mass Spectra. ESI mass spectra of all the metal complexes support the proposed structure of the complexes. The copper complex shows main peak at *m/z* 580 corresponding to the molecular weight of the complex (Figure S6). The fragmentation peaks of copper complex are observed at *m/z* 379 and 491. The molecular ion and fragmentation peaks have half intensity peaks due to isotopic distributions of copper (^{63}Cu and ^{65}Cu) [26, 27]. The spectral result shows that metal complexes are monomeric in nature and the metal to ligand ratio is 1 : 1. Nickel and zinc complexes are the same as copper, supported by analytical and spectral analysis.

3.6. EPR Spectra. The X-band EPR spectrum of the copper complex was recorded at 300 K and at 77 K using TCNE as the g marker (Figure S7). The absence of a half-field signal at 1600 G due to the $m_s = \pm 2$ transitions ruling out any Cu-Cu interaction suggests the monomeric nature of the CuL complex. The observed g values are $g_{\text{II}}(2.29) > g_{\perp}(2.11) > g_e$ (2.0027), suggesting the unpaired electron is in the d_{x2-y2} orbital (Table 2). The $g_{\text{II}}/A_{\text{II}}$ value calculated for CuL (138 cm) lies between 90 and 140 cm indicating a square planar structure around the Cu (II) ion [28–30]. The g_{II} value of 2.29 for the CuL complex indicates the covalent nature of the metal-ligand bond. The g values are related to exchange interaction coupling constant (G) by the expression $G = (g_{\text{II}} - 2.0027)/(g_{\perp} - 2.0027)$. If $G < 4$, the ligand forming the copper complex is regarded as a strong-field ligand. For the present square planar complex, $G = 2.67$ indicates that the ligand is strong field and the metal-ligand bonding in the complex is covalent [31].

The bonding parameters α^2, β^2, and γ^2 which may be regarded as covalency of the in-plane σ bond, in-plane π bond, and out-of-plane π bond, respectively, were evaluated from the following expressions [32]:

$$\alpha^2 = -\frac{A_{II}}{0.036} + (g_{\text{II}} - 2.0027) + \frac{3}{7}(g_{\perp} - 2.0027) + 0.04, \quad (4)$$

$$\beta^2 = (g_{\text{II}} - 2.0027)\frac{E}{-8\lambda\alpha^2}, \quad (5)$$

$$\gamma^2 = (g_{\perp} - 2.0027)\frac{E}{-2\lambda\alpha^2}, \quad (6)$$

where $\lambda = -828\,\text{cm}^{-1}$ for Cu(II) d^9 system and E is the electronic transition energy. The α^2 value of 0.83 for CuL demonstrates that the complex has covalent character in the ligand environment. The observed β^2 and γ^2 values indicate that there is an interaction in the in-plane π bonding between the metal ion and ligand. This is also confirmed by orbital reduction factors, K_{II} and $K_{\perp}$: $K_{\text{II}} = \alpha^2\beta^2$ and $K_{\perp} = \alpha^2\gamma^2$. In the present investigation the trend $K_{\text{II}} < K_{\perp}$ for the copper complex implies a considerable in-plane π bonding is between the metal ion and the ligand [33].

3.7. Thermal Studies. The metal complexes show gradual loss in weight due to the decomposition with increasing temperature (Figure S8). The thermogram shows four decomposition steps within the temperature range of 25–1000°C. In the first step upto 100°C, the mass loss (3–4.2%) corresponds to loss of lattice water molecule. In the second step (100–275°C), the mass loss of 22–25% corresponds to removal of the ester and methoxy groups with evolution of CO_2 gas. The third step of decomposition is noticed in the temperature range 275–450°C with loss of 28–30% due to the removal of the amino part of the ligand in the complexes. The fourth stage of decomposition occurs in the range 450–1000°C, which corresponds to the removal of the remaining part of the ligand leaving metal oxide as a residue.

3.8. DNA Binding Experiments

3.8.1. Absorption Spectroscopic Studies. All the metal complexes show intraligand ($\pi \rightarrow \pi^*$) transition in the region 270–280 nm. On addition of DNA, this band of the complexes was affected resulting in the tendency of hypochromism lying in the range 20–32% and a slight bathochromic shift in the range of 1.6-1.7 nm (Figure 2). These phenomena indicate that the complexes probably interact with CT DNA by intercalation binding mode. The extent of hypochromism is commonly consistent with the strength of intercalative interaction [34]. In order to study the binding ability of the compounds with CT DNA, the binding constant, K_b, was determined. The K_b values of the ligand ($1.23 \times 10^5\,\text{M}^{-1}$) and its copper complex ($1.00 \times 10^5\,\text{M}^{-1}$) are comparable. But the K_b values are found to be lower than those reported for typical intercalators (for ethidium bromide and $[\text{Ru(Phen)}_2(\text{dppz})]^{2+}$; the binding constants have been found to be of the order 1.4×10^6 and $>10^6\,\text{M}^{-1}$) [35]. The K_b values indicate that the binding strength of the N-alkylated salan

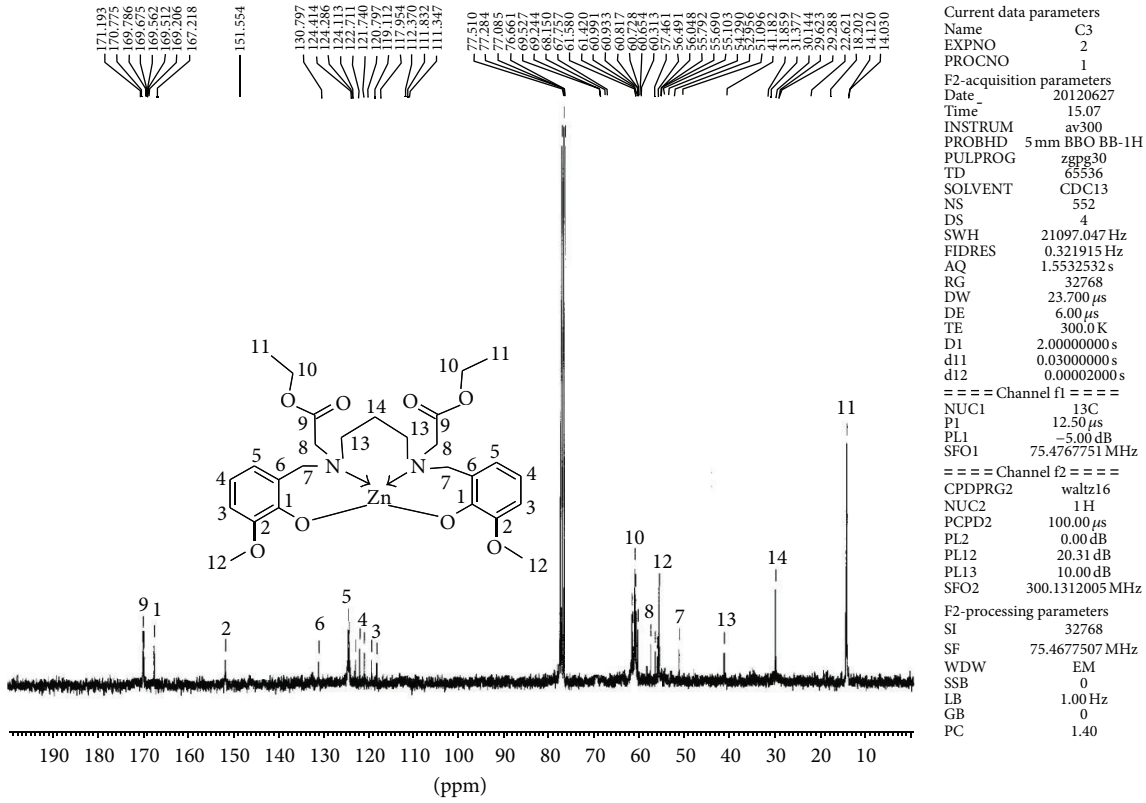

Figure 1: ^{13}C NMR spectrum of ZnL recorded in DMSO-d_6.

Table 1: Absorption and emission spectral properties of metal (II) complexes with CT DNA.

Compound	λ_{max} (nm)	Band assignments	λ_{max} (nm) Free	λ_{max} (nm) Bound	$\Delta\lambda$ (nm)	^{a}H%	$K_b \times 10^4$ (M^{-1})	$K_{app} \times 10^5$ (M^{-1})	$K_{sv} \times 10^3$ (M^{-1})	$K_{bin} \times 10^4$ (M^{-1})	n
CuL	285, 349, 527	$\pi \rightarrow \pi^*$, $^2B_{1g} \rightarrow {}^2A_{1g}$	271.5	273.2	1.7	32	10	6.25	8.44	3.08	1.159
NiL	280, 345, 553	$\pi \rightarrow \pi^*$, $^1A_{1g} \rightarrow {}^1A_{2g}$	278.1	279.7	1.6	21	5	5	6.58	1.43	1.092
ZnL	282, 350	$\pi \rightarrow \pi^*$	274.8	276.4	1.6	20	4	4.16	7.89	0.87	1.024

ligand (L) and CuL with DNA is stronger than that of salen, salan [14], NiL, and ZnL (Table 1).

3.8.2. Fluorescence Spectral Studies. The EB fluorescence displacement experiment has been widely used to investigate the interaction of metal complexes with DNA. The EB shows weak fluorescence in buffer solution. The fluorescence intensity of EB in presence of DNA can be greatly enhanced due to intercalation with DNA [36]. On addition of metal complexes (0–120 μM) to DNA-EB mixture, the metal complex competes with EB to bind with DNA. This leads to a decrease in the binding sites of DNA available for EB, and hence quenching of fluorescence intensity of EB-DNA mixture occurs (Figure 3). The quenching plot illustrates that the quenching of ethidium bromide bound to DNA by metal complexes is in agreement with the linear Stern-Volmer equation. The value of K_{sv} for CuL, NiL, and ZnL is found to be 8.44×10^3, 6.58×10^3, and 7.89×10^3, respectively. The apparent binding constant (K_{app}) values obtained for the CuL, NiL, and ZnL compounds are found to be 6.25×10^5, 5×10^5, and 4×10^5, respectively (Table 1). Furthermore, the quenching constants and binding constants calculated for the complexes suggest that the interaction of all the compounds with DNA occurs through intercalation. The DNA binding abilities of the complexes follow the order Cu(II) > Ni(II) > Zn(II), which is in conformity with the trend in DNA binding affinities obtained from absorption spectral studies.

Binding Analysis. The equilibrium binding constant and the number of binding sites can be analyzed according to the Scatchard equation [37, 38]:

$$\log \frac{I_0 - I}{I} = \log K_{bin} + n \log [Q], \quad (7)$$

where K_{bin} is the binding constant of complex with DNA and n is the number of binding sites. From the plot of log

Table 2: Spin Hamiltonian parameters of Cu(II) complex in DMSO at 300 K and 77 K.

Compound	Hyperfine constant 10^{-4} (cm^{-1})												
	A_{II}	$A_{\perp}$	A_{av}	g_{II}	$g_{\perp}$	g_{av}	g_{II}/A_{II}	K_{II}	$K_{\perp}$	α^2	β^2	γ^2	G
CuL	165	135	145	2.29	2.11	2.17	138	0.82	1.22	0.83	0.99	1.48	2.67

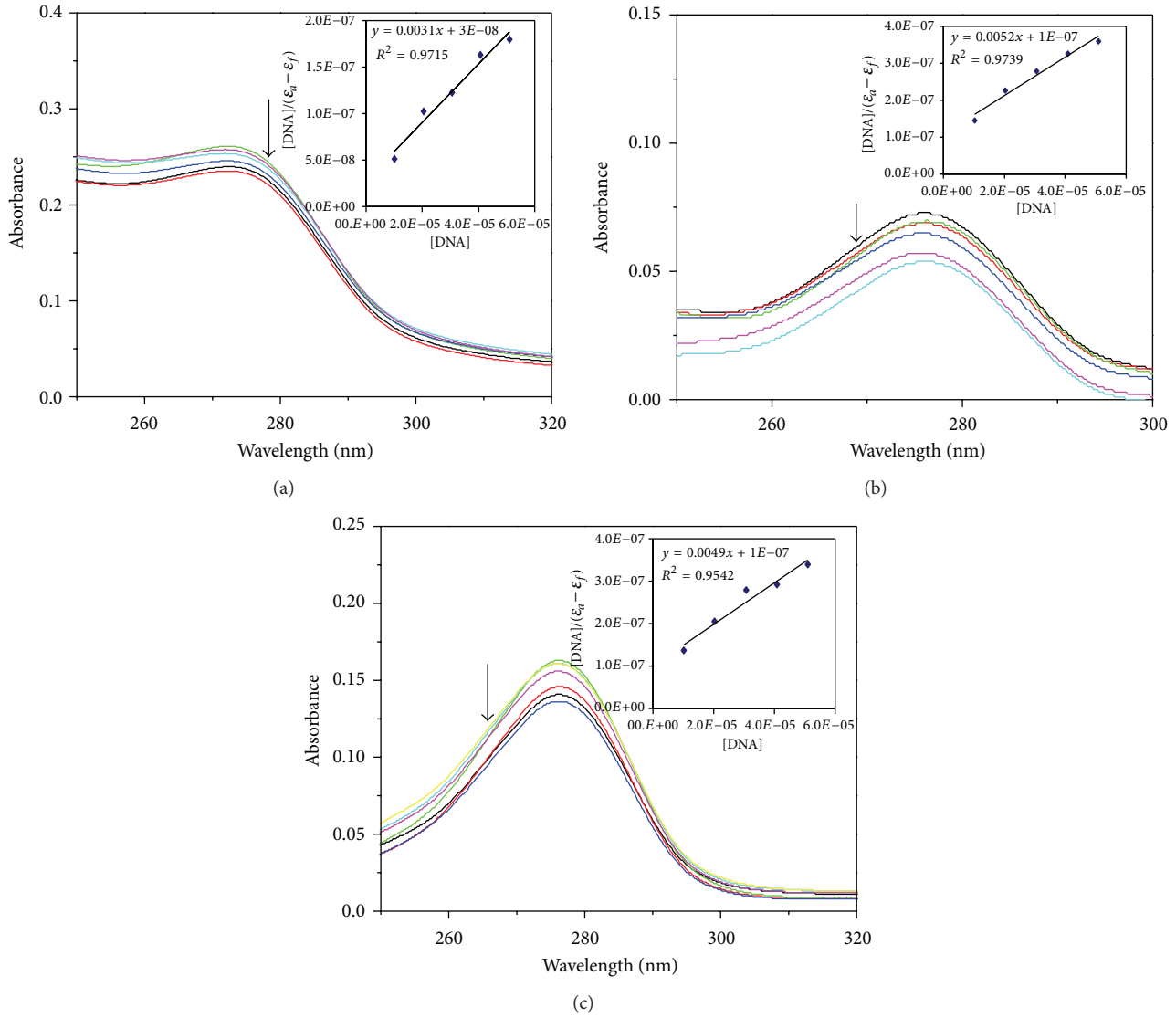

Figure 2: UV-Vis absorption spectra of (a) CuL, (b) NiL, and (c) ZnL (10 μM) in the absence and presence of increasing amounts of CT DNA; [DNA] = 0–60 μM. The arrow indicates the absorbance change upon increasing DNA concentration. The inset is a plot of [DNA]/($\varepsilon_a - \varepsilon_f$) versus [DNA].

($I_0 - I$)/I versus log[Q], the number of binding sites and binding constant have been obtained (Figure 4). The value of n is around one for all the compounds indicating the existence of only one independent class of binding sites for the metal complexes on DNA (Table 1). The values of K_{sv} and K_{bin} suggest that the complexes interact strongly with DNA.

3.8.3. Electrochemical Studies. The redox behaviour of the Cu(II) complex in DMSO was examined by means of cyclic voltammetry (potential range −1 V to +1 V) with different scan rates from 25 to 125 mVs^{-1} (Figure 5). The cyclic voltammogram shows a well-defined quasireversible peak for the redox couple Cu(III)/Cu(II) [Ep_a = 0.604 V and Ep_c = 0.260 V]. In the negative potential range copper shows irreversible cathodic peak at −0.675 V [Cu(II)/Cu(I)] with the scan rate of 100 mVs^{-1} (Table S3). The limiting peak to peak separation (ΔEp) for Cu(III)/Cu(II) process is greater than 59 mV which revealed that the couple is quasireversible. The ratio of anodic to cathodic peak current value is 1.1 demonstrating the simple

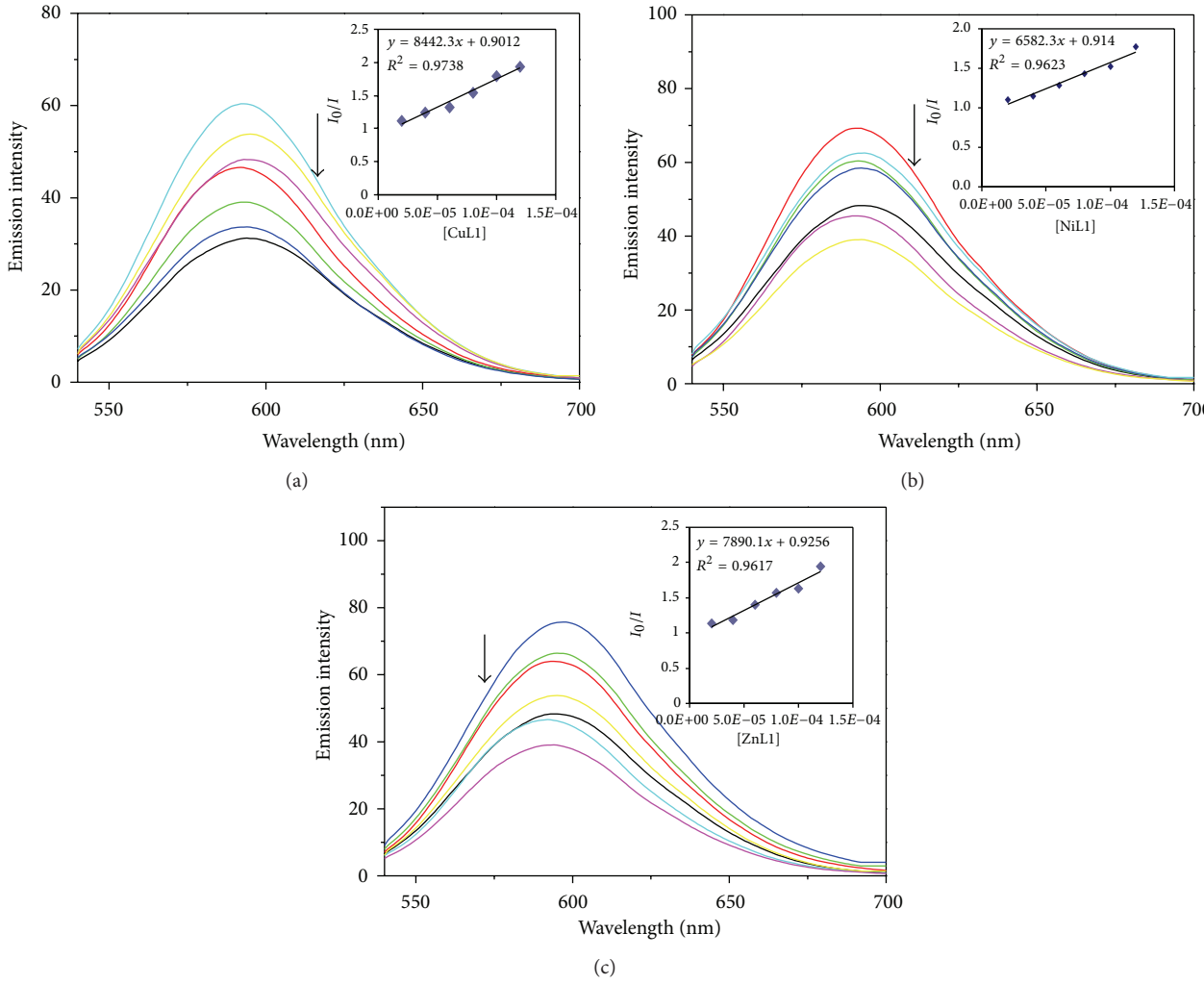

FIGURE 3: Emission spectra of ethidium-bromide-bound DNA in the presence of (a) CuL, (b) NiL, and (c) ZnL. The arrow shows the intensity change upon increasing complex concentrations. Inset shows the plot of I_0/I Vs [complex].

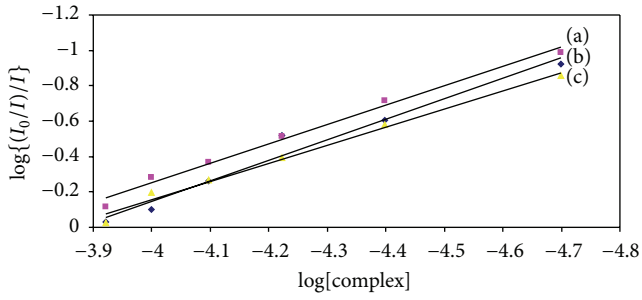

FIGURE 4: Scatchard plot of fluorescence titration of (a) CuL, (b) NiL, and (c) ZnL with CT DNA.

one-electron process. Further, the anodic peak is shifted towards positive potential value, and the cathodic peak is shifted towards negative potential with a function of scan rate 25 to 125 mVs^{-1} which supports quasireversible process.

The cyclic voltammetric technique provides information about interaction between the metal complexes and DNA. DNA is denatured in DMSO medium, so we recorded the CV of copper complex in Tris-HCl buffer containing 10% DMSO. In Buffer medium, the copper complex shows a Cu(II)/Cu(I) couple with Ep_c at −0.438 V and Ep_a at 0.137 V (Figure S9). The separations of anodic and cathodic peaks (ΔEp) are found to be 0.575 V indicating quasireversible one-electron redox process (Table S4). In the presence of CT DNA with R = 10 (R = [DNA]/[complex]) both the anodic and cathodic peak currents are decreased with shifting of potential values indicating that there exist interactions between copper complex and CT DNA. The drop of the voltammetric current in the presence of CT DNA is due to slow diffusion of the copper complex bound to CT DNA. The formal potential, $E_{1/2}$, taken as the average of Ep_c and Ep_a shifts slightly towards the positive side on binding to DNA which suggests that copper complex binds intercalatively to CT DNA [39].

3.9. DNA Cleavage Activity. The cleavage of pUC19 DNA induced by the metal complexes in the presence of H_2O_2 is shown in Figure S10. In the absence of the complex (Lane 1),

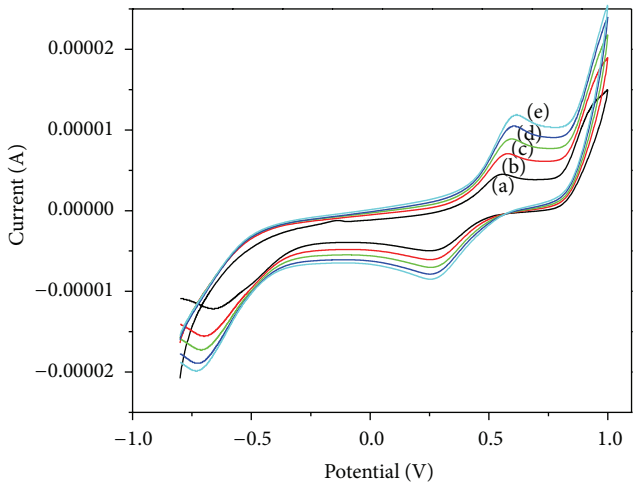

FIGURE 5: Cyclic voltammogram of CuL at different scan rates: (a) 25 mVs^{-1}, (b) 50 mVs^{-1}, (c) 75 mVs^{-1}, (d) 100 mVs^{-1}, and (e) 125 mVs^{-1}.

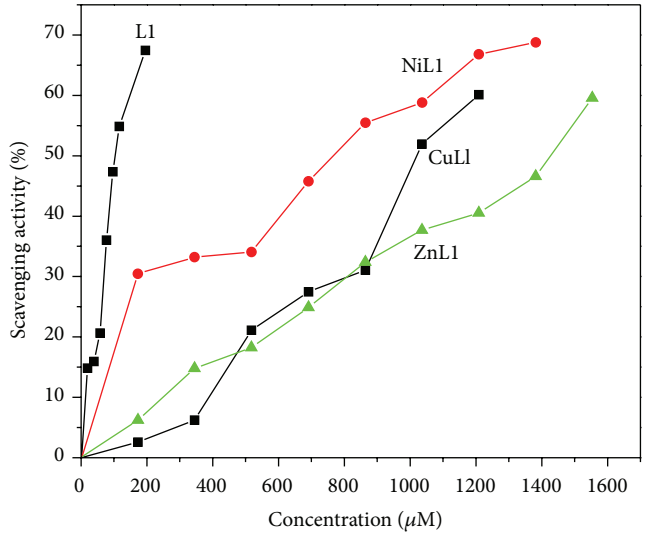

FIGURE 6: Scavenging activity of the ligand (L) and its Cu(II), Ni(II), and Zn(II) complexes at various concentrations.

DNA remains in the supercoiled form. Incubation of DNA with copper complex (Lane 2) leads to its conversion to form II and form III. This indicates that copper complex has the ability to cleave pUC19 DNA in presence of oxidant H_2O_2. The probable reason may be the oxidation of deoxyribose moiety by hydroxyl free radicals followed by the hydrolytic cleavage of the sugar phosphate backbone. The cleavage efficiency was measured in terms of the ability of the complex to convert the supercoiled form to open circular form. The ability of nickel and zinc complexes (lane 3 and lane 4) in the interconversion of supercoiled form to open circular form (form I to form II) is less when compared to the copper complex. In the absence of H_2O_2, the synthesized complexes did not show any effect towards the cleavage of DNA.

3.10. Antioxidant Property. The antioxidant activity of the ligand and the metal complexes was measured in terms of their hydrogen donating or radical scavenging capability by DPPH assay method. Upon addition of metal complexes, the reduction of DPPH radical is monitored by the decrease of the absorbance of its radical at 517 nm (Figure 6). The absorbance decreases as a result of color changes from purple to yellow as the radical is scavenged by antioxidants. The 50% inhibitory concentration (IC_{50}) values of L, CuL, NiL, and ZnL are 103, 1019, 771, and 1429 μM, respectively. The higher free radical scavenging activity of the ligand may be due to the presence of free phenolic –OH groups. The IC_{50} values of synthesized compounds are much higher than the positive control like ascorbic acid, 11.55 μM [40].

3.11. Antibacterial Activity. The *in vitro* antibacterial activities of the synthesized compounds were tested against six human pathogenic microorganisms (gram-positive bacteria: *Streptococcus pyogenes* and *Staphylococcus aureus*; gram-negative bacteria: *Escherichia Coli*, *Klebsiella mobilis, Aeromonas aquariorum*, and *Serratia marcescens*) by well diffusion method using ampicillin and amoxicillin as standards. The susceptibility of the strains of bacteria towards the present compounds was judged by measuring the size of inhibition diameter (Figure S11). The comparison of the antimicrobial activity of the synthesized compounds and the known antibiotics showed that the metal complexes were more effective than the ligand or metal salts but less active than the controls against all the bacteria tested. The bulky N-alkylated ligand on chelation to the metal cation reduces the polarity of the metal ion due to the ligand orbital overlap with the metal orbitals, resulting in a delocalization of positive charge. This increases the lipophilic character of the metal chelate and favors its permeation through the lipoid layer of the bacterial membranes. Cu(II) complex has higher antibacterial activity against *Streptococcus pyogenes* and *Escherichia Coli* than the other metal complexes. Zn(II) complex has higher activity against *Klebsiella mobilis, Aeromonas aquariorum*. Ni(II) complex is found to have moderate activity towards the bacteria tested.

4. Conclusion

Salan-type ligand containing ester groups was synthesized. The N-alkylated salan was used to prepare Cu(II), Ni(II), and Zn(II) complexes. The synthesized compounds were characterized by spectral and analytical techniques. Spectral studies reveal that the ligand coordinates to the metal ion through the phenolic –O and tertiary –N atoms. The presence of ester groups in tertiary –N leads to distortion from the regular square planar geometry of the complexes. The cyclic voltammogram of copper complex reveals that the complex exhibits well-defined quasireversible Cu(III)/Cu(II) couple along with Cu(II) irreversible process. The synthesized compounds bind to CT DNA through intercalation mode. Copper complex has been found to promote cleavage of pUC19 DNA from the super coiled form to nicked form in presence of H_2O_2. The metal complexes show higher bacterial

activity than the ligand. The ligand shows more effective free radical scavenger activity than the metal complexes.

Acknowledgments

Dr. M.A.Neelakantan wishes to thank the Department of Science and Technology, New Delhi, for providing UV-Vis spectrophotometer through funding (SR/S1/IC-08/2010). The authors thank SAIF, IIT-Bombay, for EPR measurements and CDRI-Lucknow for ESI-Mass spectrophotometer facility.

References

[1] M. Wang, L.-F. Wang, Y.-Z. Li, Q.-X. Li, Z.-D. Xu, and D.-M. Qu, "Antitumour activity of transition metal complexes with the thiosemicarbazone derived from 3-acetylumbelliferone," *Transition Metal Chemistry*, vol. 26, no. 3, pp. 307–310, 2001.

[2] M. A. Musa, M. O. F. Khan, A. Aspedon, and J. S. Cooperwood, "Synthesis and antimicrobial activity of N,N′-bis(2-hydroxylbenzyl)-1, 2-ethanediamine derivatives," *Letters in Drug Design and Discovery*, vol. 7, no. 3, pp. 165–170, 2010.

[3] M. S. Nair, S. S. Kumari, and M. A. Neelakantan, "Studies on some novel Schiff-base complexes in solution and solid state," *Journal of Coordination Chemistry*, vol. 60, no. 12, pp. 1291–1302, 2007.

[4] P. Tarasconi, S. Capacchi, G. Pelosi et al., "Synthesis, spectroscopic characterization and biological properties of new natural aldehydes thiosemicarbazones," *Bioorganic and Medicinal Chemistry*, vol. 8, no. 1, pp. 157–162, 2000.

[5] J. Charo, J. A. Lindencrona, L.-M. Carlson, J. Hinkula, and R. Kiessling, "Protective efficacy of a DNA influenza virus vaccine is markedly increased by the coadministration of a Schiff base-forming drug," *Journal of Virology*, vol. 78, no. 20, pp. 11321–11326, 2004.

[6] J. G. Muller, S. J. Paikoff, S. E. Rokita, and C. J. Burrows, "DNA modification promoted by water-soluble nickel (II) salen complexes: a switch to DNA alkylation," *Journal of Inorganic Biochemistry*, vol. 54, no. 3, pp. 199–206, 1994.

[7] S. Routier, H. Vezin, E. Lamour, J.-L. Bernier, J.-P. Catteau, and C. Bailly, "DNA cleavage by hydroxy-salicylideneethylendiamine-iron complexes," *Nucleic Acids Research*, vol. 27, no. 21, pp. 4160–4166, 1999.

[8] S. Routier, J.-L. Bernier, M. J. Waring, P. Colson, C. Houssier, and C. Bailly, "Synthesis of a functionalized salen-copper complex and its interaction with DNA," *Journal of Organic Chemistry*, vol. 61, no. 7, pp. 2326–2331, 1996.

[9] V. Selvarani, B. Annaraj, M. A. Neelakantan, S. Sundaramoorthy, and D. Velmurugan, "Synthesis, characterization and crystal structures of copper(II) and nickel(II) complexes of propargyl arm containing N_2O_2 ligands: antimicrobial activity and DNA binding," *Polyhedron*, vol. 5, pp. 74–83, 2013.

[10] D. Prema, A. V. Wiznycia, B. M. T. Scott, J. Hilborn, J. Desper, and C. J. Levy, "Dinuclear zinc(ii) complexes of symmetric Schiff-base ligands with extended quinoline sidearms," *Dalton Transactions*, no. 42, pp. 4788–4796, 2007.

[11] M. Komiyama, N. Takeda, and H. Shigekawa, "Hydrolysis of DNA and RNA by lanthanide ions: mechanistic studies leading to new applications," *Chemical Communications*, no. 16, pp. 1443–1451, 1999.

[12] M. A. Neelakantan, S. S. Marriappan, J. Dharmaraja, T. Jeyakumar, and K. Muthukumaran, "Spectral, XRD, SEM and biological activities of transition metal complexes of polydentate ligands containing thiazole moiety," *Spectrochimica Acta Part A*, vol. 71, no. 2, pp. 628–635, 2008.

[13] V. Selvarani, B. Annaraj, M. A. Neelakantan, S. Sundaramoorthy, and D. Velmurugan, "Synthesis and crystal structure of hydroxyacetophenone Schiff bases containing propargyl moiety: solvent effects on UV-visible spectra," *Spectrochimica Acta Part A*, vol. 91, pp. 329–337, 2012.

[14] P. J. K. Inba, B. Annaraj, S. Thalamuthu, and M. A. Neelakantan, "Salen, reduced salen and N-alkylated salen type compounds: spectral characterization, theoretical investigation and biological studies," *Spectrochimica Acta Part A*, vol. 104, pp. 300–309, 2013.

[15] D. D. Perrin, W. L. F. Armarego, and D. R. Perrin, *Purification of Laboratory Chemicals*, Pergamon Press, Oxford, UK, 1980.

[16] C. R. Merril, D. Goldman, S. A. Sedman, and M. H. Ebert, "Ultrasensitive stain for proteins in polyacrylamide gels shows regional variation in cerebrospinal fluid proteins," *Science*, vol. 211, no. 4489, pp. 1437–1438, 1981.

[17] M. E. Reichmann, S. A. Rice, C. A. Thomas, and P. Doty, "A further examination of the molecular weight and size of desoxypentose nucleic acid," *Journal of the American Chemical Society*, vol. 76, no. 11, pp. 3047–3053, 1954.

[18] A. Wolfe, G. H. Shimer Jr., and T. Meehan, "Polycyclic aromatic hydrocarbons physically intercalate into duplex regions of denatured DNA," *Biochemistry*, vol. 26, no. 20, pp. 6392–6396, 1987.

[19] O. Stern and M. Volmer, "On the quenching-time of fluorescence," *Physikalische Zeitschrift*, vol. 20, pp. 183–188, 1919.

[20] M. Lee, A. L. Rhodes, M. D. Wyatt, S. Forrow, and J. A. Hartley, "GC base sequence recognition by oligo(imidazolecarboxamide) and C-terminus-modified analogues of distamycin deduced from circular dichroism, proton nuclear magnetic resonance, and methidiumpropylethylenediaminetetraacetate-iron(II) footprinting studies," *Biochemistry*, vol. 32, no. 16, pp. 4237–4245, 1993.

[21] M. S. Blois, "Antioxidant properties of modified rutin esters by DPPH, reducing power, iron chelation and human low density lipoprotein assays," *Nature*, vol. 181, no. 4617, pp. 1199–1200, 1958.

[22] W. Brand-Williams, M. E. Cuvelier, and C. Berset, "Use of a free radical method to evaluate antioxidant activity," *LWT-Food Science and Technology*, vol. 28, no. 1, pp. 25–30, 1995.

[23] B.-M. Lue, N. S. Nielsen, C. Jacobsen, L. Hellgren, Z. Guo, and X. Xu, "Antioxidant properties of modified rutin esters by DPPH, reducing power, iron chelation and human low density lipoprotein assays," *Food Chemistry*, vol. 123, no. 2, pp. 221–230, 2010.

[24] M. J. Pelczar, E. C. S. Chanm, and N. R. Krieg, *Microbiology*, Blackwell Science, New York, NY, USA, 1998.

[25] A. B. P. Lever, *Inorganic Electronic Spectroscopy*, Elsevier, New York, NY, USA, 2nd edition, 1984.

[26] A. Matsumoto, T. Fukumoto, H. Adachi, and H. Watarai, "Electrospray ionization mass spectrometry of metal complexes. Gas phase formation of a binuclear copper(II)-5-Br-PADAP complex," *Analytica Chimica Acta*, vol. 390, no. 1–3, pp. 193–199, 1999.

[27] W. A. Alves, G. Cerchiaro, A. Paduan-Filho, D. M. Tomazela, M. N. Eberlin, and A. M. Da Costa Ferreira, "Infinite zig-zag and

cyclic-tetranuclear isomeric imidazolate-bridged polynuclear copper(II) complexes: magnetic properties, catalytic activity and electrospray mass and tandem mass spectrometry characterization," *Inorganica Chimica Acta*, vol. 358, no. 13, pp. 3581–3591, 2005.

[28] U. Sakaguchi and A. W. Addison, "Spectroscopic and redox studies of some copper(II) complexes with biomimetic donor atoms: implications for protein copper centres," *Journal of the Chemical Society, Dalton Transactions*, no. 4, pp. 600–608, 1979.

[29] V. P. Daniel, B. Murukan, B. S. Kumari, and K. Mohanan, "Synthesis, spectroscopic characterization, electrochemical behaviour, reactivity and antibacterial activity of some transition metal complexes with 2-(N-salicylideneamino)-3-carboxyethyl-4,5-dimethylthiophene," *Spectrochimica Acta Part A*, vol. 70, no. 2, pp. 403–410, 2008.

[30] S. M. D. M. Romanowski, F. Tormena, V. A. Dos Santos, M. D. F. Hermann, and A. S. Mangrich, "Solution studies of copper(II) complexes as a contribution to the study of the active site of galactose oxidase," *Journal of the Brazilian Chemical Society*, vol. 15, no. 6, pp. 897–903, 2004.

[31] R. L. Dutta and A. Syamal, *Elements of Magnetochemistry*, Affliated East-West Press, New Delhi, India, 2nd edition, 1993.

[32] R. Neiman and D. Kivelson, "ESR line shapes in glasses of copper complexes," *The Journal of Chemical Physics*, vol. 35, no. 1, pp. 149–155, 1961.

[33] B. J. Hathaway, "The evidence for "out-of-the-plane" bonding in axial complexes of the copper(II) ion," *Structure and Bonding*, vol. 14, pp. 49–67, 1973.

[34] L.-F. Tan, H. Chao, H. Li et al., "Synthesis, characterization, DNA-binding and photocleavage studies of $[Ru(bpy)2(PPIP)]^{2+}$ and $[Ru(phen)2(PPIP)]^{2+}$," *Journal of Inorganic Biochemistry*, vol. 99, no. 2, pp. 513–520, 2005.

[35] M. J. Waring, "Complex formation between ethidium bromide and nucleic acids," *Journal of Molecular Biology*, vol. 13, no. 1, pp. 269–282, 1965.

[36] F. J. Meyer-Almes and D. Porschke, "Mechanism of intercalation into the DNA double helix by ethidium," *Biochemistry*, vol. 32, no. 16, pp. 4246–4253, 1993.

[37] J. R. Lakowicz, *Fluorescence Quenching: Theory and Applications. Principles of Fluorescence Spectroscopy*, Kluwer Academic/Plenum Publishers, New York, NY, USA, 1999.

[38] X.-Z. Feng, Z. Lin, L.-J. Yang, C. Wang, and C.-L. Bai, "Investigation of the interaction between acridine orange and bovine serum albumin," *Talanta*, vol. 47, no. 5, pp. 1223–1229, 1998.

[39] J. Annaraj, S. Srinivasan, K. M. Ponvel, and P. R. Athappan, "Mixed ligand copper(II) complexes of phenanthroline/bipyridyl and curcumin diketimines as DNA intercalators and their electrochemical behavior under Nafion and clay modified electrodes," *Journal of Inorganic Biochemistry*, vol. 99, no. 3, pp. 669–676, 2005.

[40] T. Noipa, S. Srijaranai, T. Tuntulani, and W. Ngeontae, "New approach for evaluation of the antioxidant capacity based on scavenging DPPH free radical in micelle systems," *Food Research International*, vol. 44, no. 3, pp. 798–806, 2011.